Progress In Electromagnetics Research, PIER 65, 137–155, 2006

AN ANALYTICAL INVESTIGATION OF THE RADIATION CHARACTERISTICS OF INFINITESIMAL DIPOLE ANTENNA EMBEDDED IN PARTIALLY REFLECTIVE SURFACES TO OBTAIN HIGH DIRECTIVITY

A. Pirhadi and M. Hakkak

Faculty of Engineering
Department of Electrical Engineering
Tarbiat Modares University (TMU)
Tehran, Iran

Abstract—The far-field radiation characteristics of an infinitesimal dipole embedded between two partially reflective surfaces (PRS) to obtain high directivity are studied analytically. The analysis is based on integral summation of spectral radiation fields of the source in cylindrical coordinate, so that we can find the effects of transmission and reflection coefficients of PRS on all components of primary radiation source. The analysis shows that due to the existence of TE_z and TM_z modes for horizontal dipole source, the effects of PRSs are different for each mode. Also, this study shows that by adjusting the spacing of the plates, it is possible to achieve high directive multibeam patterns.

1. INTRODUCTION

Two conventional strategies to obtain high directivity in antenna configurations are using large aperture antennas, such as horn and reflector antennas, and using arrays of small radiation sources. However, there are many problems related to these configurations, such as weight, geometry, construction and feeding network. High directive resonator antennas, which have been recently introduced to obtain high directivity from a small radiation sources [1, 3], are new candidates. Two methods for the design of such structures are;

- Using small radiation source embedded in defected 1-D or 2-D electromagnetic bandgap structures (EBG) [2–7].

- Using a Fabry-Perot cavity phenomenon excited by small radiation source [8–10].

Different methods of analysis of the two mentioned configurations are introduced. To analyze the first configuration a suitable EBG structure is excited by a plane wave to determine its bandgap [7] and then a suitable defect in the structure is exerted to achieve a resonance frequency in the bandgap region. A small radiation source placed in the structure would then yield highly directive radiation pattern at the resonance frequency. In this method the EBG structure is analyzed separately and after describing its characteristics, it is used to analyze the radiation of the source. In the second configuration, also its behavior when excited by a plane wave from their inside and outside is perused, but instead of EBG structure the small radiation source is embedded between two PRS or mirrors. In addition to this method, to achieve more accurate characteristics of structure the method based on transmission line model is used in [11–13]. In all of these methods the authors don't consider the direct effects of PRS on the electromagnetic field components of primary small radiation source. In this paper to study the effects of PRS on the electromagnetic radiation fields of arbitrary source, we examine the effects of such structure on the far field characteristics of a point source that is embedded in it. By spectral representation of radiation fields that is suitable for analyzing of multi-layer media and using far field approximation of Maxwell equations we can provide general formulation to extract the far field radiation characteristics of arbitrary source embedded in the structure.

2. SPECTRAL REPRESENTATION OF ELECTROMAGNETIC RADIATION FIELDS OF AN INFINITESIMAL DIPOLE

A suitable method to analyze layered media is the spectral representation of electromagnetic fields. By using the Sommerfeld identity the spherical radiated field by the source can be transformed into an integral summation of plane waves in cylindrical coordinate. Therefore, it is possible to impose the reflection and transmission effects of the plates and layers on the radiation fields [14].

2.1. Longitudinal Field Components of an Infinitesimal Dipole in Free Space

The spectral representation of transverse field components are derived from the spectral representation of longitudinal field components $\tilde{E}_z$ and $\tilde{H}_z$ [14].

$$\tilde{E}_s(k_\rho) = \frac{1}{k_\rho^2}\left[\nabla_s \frac{\partial \tilde{E}_z}{\partial z} - j\omega\mu\,\hat{z}\times\nabla_s\tilde{H}_z\right] \quad (1)$$

$$\tilde{H}_s(k_\rho) = \frac{1}{k_\rho^2}\left[\nabla_s \frac{\partial \tilde{H}_z}{\partial z} + j\omega\varepsilon\,\hat{z}\times\nabla_s\tilde{E}_z\right] \quad (2)$$

where $k_\rho^2 = k^2 - k_{0z}^2$. Therefore, at first it is necessary to obtain the spectral representation of longitudinal field components. Using the Dyadic Green's Function approach, the electromagnetic fields of infinitesimal electric dipole are given by [15]

$$E(r) = j\omega\mu\left(\bar{\bar{I}} + \frac{\nabla\nabla}{k^2}\right).\hat{\alpha}\,Il\frac{e^{jkr}}{4\pi r} \quad \text{and} \quad H(r) = \nabla\times\hat{\alpha}\,Il\frac{e^{jkr}}{4\pi r} \quad (3)$$

where Il is the current moment, $\hat{\alpha}$ is its direction and $k = \omega\sqrt{\varepsilon\mu}$. From (3) the electric and magnetic z components of different infinitesimal electric dipoles are shown in Table 1.

Table 1. Longitudinal field components of infinitesimal electric dipole.

Infinitesimal Electric Dipole	E_z	H_z	Modes
z-directed	$\frac{j\omega\mu\,Il}{4\pi}(1+\frac{1}{k^2}\frac{\partial^2}{\partial z^2})\,\frac{e^{jkr}}{r}$	——	TM_z
x-directed	$\frac{j\omega\mu\,Il}{4\pi\,k^2}\frac{\partial^2}{\partial z\partial \mathrm{x}}\left(\frac{e^{jkr}}{r}\right)$	$-\frac{Il}{4\pi}\frac{\partial}{\partial y}(\frac{e^{jkr}}{r})$	TM_z and TE_z
y-directed	$\frac{j\omega\mu\,Il}{4\pi\,k^2}\frac{\partial^2}{\partial z\partial y}\left(\frac{e^{jkr}}{r}\right)$	$\frac{Il}{4\pi}\frac{\partial}{\partial x}(\frac{e^{jkr}}{r})$	TM_z and TE_z

Using the Sommerfeld identity

$$\frac{e^{jkr}}{r} = \frac{j}{2}\int_{\infty}^{+\infty} dk_\rho \frac{k_\rho}{k_{0z}} H_0^{(1)}(k_\rho\rho)\,e^{jk_{0z}|z|} \quad (4)$$

with the results of Table 1, we can find integral representations of longitudinal components, shown in Table 2. Also the electromagnetic fields versus their spectral forms are represented as

$$E(r) = \int_{-\infty}^{+\infty} dk_\rho\,\tilde{E}(k_\rho, r) \quad \text{and} \quad H(r) = \int_{-\infty}^{+\infty} dk_\rho\,\tilde{H}(k_\rho, r) \quad (5)$$

where $\tilde{E}$ and $\tilde{H}$ are spectral representation of E and H. Comparing results of Table 2 and (5), we conclude that the spectral representations

Table 2. Integral representation of the longitudinal field components of infinitesimal electric dipole.

	Longitudinal Components
z-directed electric dipole	$E_z = -\frac{Il}{8\pi\omega\varepsilon_0} \int_{-\infty}^{+\infty} dk_\rho \frac{k_\rho^3}{k_{0z}} H_1^1(k_\rho\rho)\, e^{jk_{0z}\lvert z\rvert}$ $H_z = 0$
x-directed electric dipole	$E_z = \pm j \frac{Il}{8\pi\omega\varepsilon_0} \cos(\phi) \int_{-\infty}^{+\infty} dk_\rho\, k_\rho^2\, H_1^1(k_\rho\rho)\, e^{jk_{0z}\lvert z\rvert}$ $H_z = j \frac{Il}{8\pi} \sin(\phi) \int_{-\infty}^{+\infty} dk_\rho \frac{k_\rho^2}{k_{0z}} H_1^1(k_\rho\rho)\, e^{jk_{0z}\lvert z\rvert}$
y-directed electric dipole	$E_z = \pm j \frac{Il}{8\pi\omega\varepsilon_0} \sin(\phi) \int_{-\infty}^{+\infty} dk_\rho\, k_\rho^2\, H_1^1(k_\rho\rho)\, e^{jk_{0z}\lvert z\rvert}$ $H_z = -j \frac{Il}{8\pi} \cos(\phi) \int_{-\infty}^{+\infty} dk_\rho \frac{k_\rho^2}{k_{0z}} H_1^1(k_\rho\rho)\, e^{jk_{0z}\lvert z\rvert}$

of longitudinal field components equal to integrands of integrals of Table 2. Also, from duality theorem the electromagnetic field components of magnetic dipole can be obtained by the replacement $\bar{E} \to \bar{H}$, $\bar{H} \to -\bar{E}$ and $\mu \leftrightarrow \varepsilon$. By having the spectral forms of longitudinal components (Table 2) and (1) we can find the spectral representation of transverse components of the dipole fields.

3. RADIATION FROM INFINITESIMAL DIPOLE ANTENNA EMBEDDED IN PARTIALLY REFLECTIVE SURFACE

Configuration of the problem is shown in Figure 1. The primary radiation source can be vertical/horizontal infinitesimal electric or magnetic dipole. The two layers that the infinitesimal dipole is embedded between them are partially reflective surfaces with transmission and reflection coefficients t and r, respectively. Our purpose is to derive the far field radiation characteristics of the dipole in the presence of these surfaces.

Using an integral representation of the fields, the field components in each region of Figure 1 are represented as superposition of integral summations of incoming and outgoing plane waves. By invoking

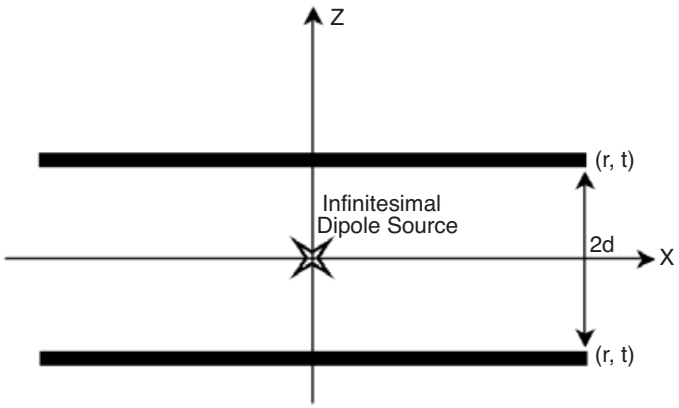

Figure 1. High directive resonance antenna structure.

the boundary conditions at the PRS locations, the amplitudes of these plane waves can be calculated. Without loss of generality, the following formulations are given for the x-directed infinitesimal electric dipole. We denote the region between plates as Region 0, and the region outside the plates as Region 1. From the results of Table 2 and equations $(1, 2)$, the fields in both regions may be expressed as follows [16], where m denotes 0 or 1:

$$E_z = \cos(\phi)\int_{-\infty}^{+\infty} dk_\rho H_1^1(k_\rho\rho)\left\{\pm E_{xed}e^{jk_{mz}|z|} + E_m^+ e^{jk_{mz}z} + E_m^- e^{-jk_{mz}z}\right\} \quad (6a)$$

$$E_\rho = \cos(\phi)\int_{-\infty}^{+\infty} dk_\rho H_1^{1'}(k_\rho\rho)\frac{jk_{mz}}{k_\rho}\left\{E_{xed}e^{jk_{mz}|z|} + E_m^+ e^{jk_{mz}z} - E_m^- e^{-jk_{mz}z}\right\}$$

$$+\cos(\phi)\int_{-\infty}^{+\infty} dk_\rho H_1^1(k_\rho\rho)\frac{j\omega\mu_m}{k_\rho^2\rho}\left\{H_{exd}e^{jk_{mz}|z|} + H_m^+ e^{jk_{mz}z} + H_m^- e^{-jk_{mz}z}\right\} \quad (6b)$$

$$E_\phi = [-\sin(\phi)]\int_{-\infty}^{+\infty} dk_\rho H_1^1(k_\rho\rho)\frac{jk_{mz}}{k_\rho^2\rho}\left\{E_{xed}e^{jk_{mz}|z|} + E_m^+ e^{jk_{mz}z} - E_m^- e^{-jk_{mz}z}\right\}$$

$$+\sin(\phi)\int_{-\infty}^{+\infty} dk_\rho H_1^{1'}(k_\rho\rho)\frac{-j\omega\mu_m}{k_\rho}\left\{H_{exd}e^{jk_{mz}|z|} + H_m^+ e^{jk_{mz}z} + H_m^- e^{-jk_{mz}z}\right\} \quad (6c)$$

$$H_z = \sin(\phi)\int_{-\infty}^{+\infty} dk_\rho H_1^1(k_\rho\rho)\left\{H_{xed}e^{jk_{mz}|z|} + H_m^+ e^{jk_{mz}z} + H_m^- e^{-jk_{mz}z}\right\} \quad (7a)$$

$$H_\rho = \sin(\phi)\int_{-\infty}^{+\infty} dk_\rho H_1^{1'}(k_\rho\rho)\frac{jk_{mz}}{k_\rho}\left\{\pm H_{exd}e^{jk_{mz}|z|} + H_m^+ e^{jk_{mz}z} - H_m^- e^{-jk_{mz}z}\right\}$$
$$+[-\sin(\phi)]\int_{-\infty}^{+\infty} dk_\rho H_1^1(k_\rho\rho)\frac{-j\omega\varepsilon_m}{k_\rho^2\rho}\left\{\pm E_{xed}e^{jk_{mz}|z|} + E_m^+ e^{jk_{mz}z} + E_m^- e^{-jk_{mz}z}\right\} \quad (7b)$$

$$H_\phi = \cos(\phi)\int_{-\infty}^{+\infty} dk_\rho H_1^1(k_\rho\rho)\frac{jk_{mz}}{k_\rho^2\rho}\left\{\pm H_{xed}e^{jk_{mz}|z|} + H_m^+ e^{jk_{mz}z} - H_m^- e^{-jk_{mz}z}\right\}$$
$$+\cos(\phi)\int_{-\infty}^{+\infty} dk_\rho H_1^{1'}(k_\rho\rho)\frac{j\omega\varepsilon_m}{k_\rho}\left\{\pm E_{xed}e^{jk_{mz}|z|} + E_m^+ e^{jk_{mz}z} + E_m^- e^{-jk_{mz}z}\right\} \quad (7c)$$

In the above formulas $E_{xed}=jIlk_\rho^2/8\pi\omega\varepsilon_m$ and $H_{exd}=jIlk_\rho^2/8\pi k_{mz}$. It is seen that each transverse component includes two terms from longitudinal components E_z and H_z as TE_z and TM_z waves, respectively. Considering boundary condition due to reflection and transmission of PRS for horizontal and vertical (TM_z and TE_z) components, we have

$$r^{TM} = \frac{E_{\mathrm{r}}^{||}}{E_{\mathrm{i}}^{||}} = \frac{-E_0^- e^{-jk_{0z}d}}{E_0^+ e^{jk_{0z}d} + E_{xed}e^{jk_{0z}d}} \quad Z = d, m = 0 \quad (8a)$$

$$r^{TM} = \frac{E_r^{||}}{E_i^{||}} = \frac{E_0^+ e^{-jk_{0z}d}}{-E_0^- e^{jk_{0z}d} + E_{xed}e^{jk_{0z}}} \quad Z = -d, m = 0 \quad (8b)$$

From (8a, 8b), we find

$$E_0^+ = \frac{r^{TM}e^{j2dk_{0z}}}{1 - r^{TM}e^{j2dk_{0z}}}E_{xed} \quad (9a)$$

$$E_0^- = \frac{-r^{TM}e^{j2dk_{0z}}}{1 - r^{TM}e^{j2dk_{0z}}}E_{xed} \quad (9b)$$

For Region 1 only the outgoing wave remains, therefore

$$t^{TM} = \frac{E_t^{\parallel}}{E_i^{\parallel}} \frac{E_1^+ e^{jk_{0z}d}}{E_0^+ e^{jk_{0z}d} + E_{xed} e^{jk_{0z}d}} \quad z = d,\ m = 1 \tag{10a}$$

$$t^{TM} = \frac{E_t^{\parallel}}{E_i^{\parallel}} \frac{-E_1^- e^{jk_{0z}d}}{-E_0^+ e^{jk_{0z}d} + E_{xed} e^{jk_{0z}d}} \quad z = -d,\ m = 1 \tag{10b}$$

From (10a, 10b)

$$E_1^+ = \frac{t^{TM}}{1 - r^{TM} e^{j2dk_{0z}}} E_{xed}; \quad Z > d \tag{11a}$$

$$E_1^- = \frac{-t^{TM}}{1 - r^{TM} e^{j2dk_{0z}}} E_{xed}; \quad Z < -d \tag{11b}$$

Using similar procedure, for TE waves we have
For Region 0

$$H_0^+ = \frac{r^{TE} e^{j2dk_{0z}}}{1 - r^{TE} e^{j2dk_{0z}}} H_{xed} \tag{12a}$$

$$H_0^- = \frac{r^{TE} e^{j2dk_{0z}}}{1 - r^{TE} e^{j2dk_{0z}}} H_{xed} \tag{12b}$$

and for Region 1

$$H_1^+ = \frac{t^{TE}}{1 - r^{TE} e^{j2dk_{0z}}} H_{xed}; \quad Z > d \tag{13a}$$

$$H_1^- = \frac{t^{TE}}{1 - r^{TE} e^{j2dk_{0z}}} H_{xed}; \quad Z < -d \tag{13b}$$

3.1. Far Field of Longitudinal Field Components

To find the representation of the radiation fields it is necessary to study the fields only in $z > d$ and $z < -d$ regions. Therefore, using the results of (11) and (13) for $z > d$ the longitudinal components of electromagnetic fields (6a, 7a) become

$$E_z = \cos(\phi) \int_{-\infty}^{+\infty} dk_\rho\ E_{xed} H_1^1(k_\rho \rho) \frac{1 + r^{TM}}{1 - r^{TM} e^{j2dk_{0z}}}\ e^{jk_{0z}z} \tag{14}$$

$$H_z = \sin(\phi) \int_{-\infty}^{+\infty} dk_\rho H_{xed} H_1^1(k_\rho \rho)\ \frac{1 + r^{TE}}{1 - r^{TE} e^{j2dk_{0z}}} e^{jk_{0z}z} \tag{15}$$

It is more expedient to expand (11a) and (13a) by geometrical series and evaluate the integrals (14) and (15) term by term.

$$E_z = \cos(\phi) \sum_{n=0}^{+\infty} \left\{ \int_{-\infty}^{+\infty} dk_\rho E_{xed} H_1^1(k_\rho \rho)(1+r^{TM})(r^{TM})^n e^{jk_{0z}(z+2nd)} \right\} \quad (16)$$

$$H_z = \sin(\phi) \sum_{n=0}^{+\infty} \left\{ \int_{-\infty}^{+\infty} dk_\rho H_{xed} H_1^1(k_\rho \rho)(1+r^{TE})(r^{TE})^n e^{jk_{0z}(z+2nd)} \right\} \quad (17)$$

In the following, for a specific frequency and any incident angle of plane waves to PRS we assume that r^{TE} *and* r^{TM} are constant. This assumption can be obtained by a suitable design of frequency selective surface (FSS) for PRS. Equations (16) and (17) would then simplify to

$$E_z = \cos(\phi) \sum_{n=0}^{+\infty} \left\{ (1+r^{TM})(r^{TM})^n \int_{-\infty}^{+\infty} dk_\rho E_{xed} H_1^1(k_\rho \rho)\, e^{jk_{0z}(z+2nd)} \right\} \quad (18)$$

$$H_z = \sin(\phi) \sum_{n=0}^{+\infty} \left\{ (1+r^{TE})(r^{TE})^n \int_{-\infty}^{+\infty} dk_\rho H_{xed} H_1^1(k_\rho \rho) e^{jk_{0z}(z+2nd)} \right\} \quad (19)$$

Because of the similarity of integral parts of E_z and H_z in (18) and (19) to E_z and H_z of the x-directed infinitesimal electric dipole located at $z = -2nd$ in free space, their far-field forms are equal, too. From (3) the longitudinal far-field components of x-directed infinitesimal electric dipole, are given by

$$E_z(r,\, \theta,\, \phi) \;=\; \frac{-j\omega\mu\, Il}{4\pi} [\sin(\theta)\cos(\theta)\cos(\phi)]\, \frac{e^{jkr}}{r}\, e^{-jk\hat{r}.\vec{r}'} \quad (20)$$

$$H_z(r,\, \theta,\, \phi) \;=\; \frac{-jk\, Il}{4\pi} [\sin(\theta)\sin(\phi)]\, \frac{e^{jkr}}{r}\, e^{-jk\hat{r}.\vec{r}'} \quad (21)$$

Therefore, the far field representation of each term of (18) and (19)

becomes

$$E_z(r,\,\theta,\,\phi) \;=\; \frac{-j\omega\mu\, Il}{4\pi}(1+r^{TM})(r^{TM})^n \\ [\sin(\theta)\cos(\theta)\cos(\phi)]\,\frac{e^{jkr}}{r}e^{j2ndk\cos(\theta)} \tag{22}$$

$$H_z(r,\,\theta,\,\phi) \;=\; \frac{-jk\, Il}{4\pi}(1+r^{TE})(r^{TE})^n \\ [\sin(\theta)\sin(\phi)]\,\frac{e^{jkr}}{r}e^{j2ndk\cos(\theta)} \tag{23}$$

3.2. Far Field of Transverse Field Components

Letting $\nabla = \nabla_s + \hat{z}\frac{\partial}{\partial z}$ where the subscript s indicates transverse to the z-direction, Maxwell's equations become

$$\left(\nabla_s + \hat{z}\frac{\partial}{\partial z}) \times (E_s + \hat{z}E_z\right) \;=\; j\omega\mu(H_s + \hat{z}H_z) \tag{24}$$

$$\left(\nabla_s + \hat{z}\frac{\partial}{\partial z}) \times (H_s + \hat{z}H_z\right) \;=\; -j\omega\varepsilon(E_s + \hat{z}E_z) \tag{25}$$

After classification the longitudinal and transverse components in (20) and (21) and some simplification we have

$$\left(k^2 + \frac{\partial^2}{\partial z^2}\right) E_S \;=\; \nabla_s(\frac{\partial}{\partial z}E_z) - j\omega\mu\,\hat{z}\times\nabla H_z \tag{26}$$

$$\left(k^2 + \frac{\partial^2}{\partial z^2}\right) H_S \;=\; \nabla_s(\frac{\partial}{\partial z}H_z) + j\omega\varepsilon\,\hat{z}\times\nabla E_z \tag{27}$$

The general far field form of the field components in (26) and (27) is $F(r,\,\theta,\,\phi) = f(\theta,\,\phi)\frac{e^{jkr}}{r}$. Normally, in the far field expressions, the terms $\frac{1}{r^n};\ n = 2,\,3,\,\ldots$ are ignored [16]. Using these assumptions the derivative terms in (26) and (27) are replaced by (See Appendix A):

$$\frac{\partial^2}{\partial x\partial z}(\bullet) \;=\; -k^2\sin(\theta)\cos(\theta)\cos(\phi)(\bullet) \tag{28}$$

$$\frac{\partial^2}{\partial y\partial z}(\bullet) \;=\; -k^2\sin(\theta)\cos(\theta)\sin(\phi)(\bullet) \tag{29}$$

$$\frac{\partial^2}{\partial z^2}(\bullet) \;=\; -k^2\cos^2(\theta)(\bullet) \tag{30}$$

$$\frac{\partial}{\partial x}(\bullet) \;=\; jk\sin(\theta)\cos(\phi)(\bullet) \tag{31}$$

$$\frac{\partial}{\partial y}(\bullet) = jk\sin(\theta)\sin(\phi)(\bullet) \tag{32}$$

Therefore, using (28)–(32) with (26) and (27) the transverse field components become

$$E_x = -\frac{\cos(\theta)\,\cos(\phi)}{\sin(\theta)}E_z - \frac{\omega\mu}{k}\frac{\sin(\phi)}{\sin(\theta)}H_z \tag{33}$$

$$E_y = -\frac{\cos(\theta)\,\sin(\phi)}{\sin(\theta)}E_z + \frac{\omega\mu}{k}\frac{\cos(\phi)}{\sin(\theta)}H_z \tag{34}$$

$$H_x = -\frac{\cos(\theta)\,\cos(\phi)}{\sin(\theta)}H_z + \frac{\omega\varepsilon}{k}\frac{\sin(\phi)}{\sin(\theta)}E_z \tag{35}$$

$$H_y = -\frac{\cos(\theta)\,\sin(\phi)}{\sin(\theta)}H_z - \frac{\omega\varepsilon}{k}\frac{\cos(\phi)}{\sin(\theta)}E_z \tag{36}$$

Also, the far-field spherical components of the radiation fields can be written as

$$E_r = 0 \tag{37}$$

$$E_\theta = \frac{E_z}{\sin(\theta)} \tag{38}$$

$$E_\phi = \frac{\omega\mu}{k}\frac{H_z}{\sin(\theta)} \tag{39}$$

$$H_r = 0 \tag{40}$$

$$H_\theta = -\frac{H_z}{\sin(\theta)} \tag{41}$$

$$H_\phi = -\frac{\omega\varepsilon}{k}\frac{E_z}{\sin(\theta)} \tag{42}$$

Now, using E_z and H_z from (22, 23) in (37–42) we obtain

$$E_r = 0 \tag{43}$$

$$E_\theta = \frac{j\omega\mu\, Il}{4\pi}\left[(1+r^{TM})(r^{TM})^n\cos(\theta)\cos(\phi)\right]\frac{e^{jkr}}{r}e^{j2ndk\cos(\theta)} \tag{44}$$

$$E_\phi = \frac{j\omega\mu\, Il}{4\pi}\left[(1+r^{TE})(r^{TE})^n[-\sin(\phi)\right]\frac{e^{jkr}}{r}e^{j2ndk\cos(\theta)} \tag{45}$$

$$H_r = 0 \tag{46}$$

$$H_\theta = \frac{jkIl}{4\pi}\left[(1+r^{TE})(r^{TE})^n\sin(\phi)\right]\frac{e^{jkr}}{r}e^{j2ndk\cos(\theta)} \tag{47}$$

$$H_\phi = \frac{jkIl}{4\pi}\left[(1+r^{TM})(r^{TM})^n\cos(\theta)\cos(\phi)\right]\frac{e^{jkr}}{r}e^{j2ndk\cos(\theta)} \tag{48}$$

Finally, the total radiation fields of the structure from all summation terms become

$$E_r^{total} = 0 \tag{49}$$

$$E_\theta^{total} = \frac{j\omega\mu\, Il}{4\pi}\frac{1+r^{TM}}{1-r^{TM}e^{j2dk\cos(\theta)}}\cos(\theta)\cos(\phi)\frac{e^{jkr}}{r} \tag{50}$$

$$E_\phi^{total} = \frac{j\omega\mu\, Il}{4\pi}\frac{1+r^{TE}}{1-r^{TE}e^{j2dk\cos(\theta)}}[-\sin(\phi)]\frac{e^{jkr}}{r} \tag{51}$$

$$H_r^{total} = 0 \tag{52}$$

$$H_\theta^{total} = \frac{jk\, Il}{4\pi}\frac{1+r^{TE}}{1-r^{TE}e^{j2dk\cos(\theta)}}\sin(\phi)\frac{e^{jkr}}{r} \tag{53}$$

$$H_\phi^{total} = \frac{jk\, Il}{4\pi}\frac{1+r^{TM}}{1-r^{TM}e^{j2dk\cos(\theta)}}\cos(\theta)\cos(\phi)\frac{e^{jkr}}{r} \tag{54}$$

4. DIRECTIVITY OF THE STRUCTURE

Using (49)–(54) the Pointing vector becomes

$$\vec{S} = \omega\mu\, k(\frac{Il}{4\pi\, r})^2\ \left[A(\theta)\sin^2(\phi) + B(\theta)\cos^2(\phi)\cos^2(\theta)\right]\hat{r} = S_r\hat{r} \tag{55}$$

where

$$A(\theta)=\frac{\left|1+r^{TE}\right|^2}{\left|1-r^{TE}e^{j2dk\cos(\theta)}\right|^2} \quad \text{and} \quad B(\theta)=\frac{\left|1+r^{TM}\right|^2}{\left|1-r^{TM}e^{j2dk\cos(\theta)}\right|^2} \tag{56}$$

The radiation intensity of the structure for upper half space will be:

$$U_{av} = \frac{P_{rad}}{4\pi} = \frac{\oiint_S \frac{1}{2}r^2 Re(\vec{S}).\vec{ds}}{4\pi} \tag{57}$$

which after some simplification yields

$$U_{av} = \frac{\omega\mu\, k}{8}(\frac{Il}{4\pi})^2\int_0^{\pi/2}\left[A(\theta) + B(\theta)\cos^2(\theta)\right]\sin(\theta)d\theta \tag{58}$$

Because of the symmetrical property of the structure, (58) must be multiplied by 2 for the whole space. Therefore, the directivity of the structure becomes

$$D(\theta,\, \phi) = 4\frac{A(\theta)\sin^2(\phi) + B(\theta)\cos^2(\phi)\cos^2(\theta)}{\displaystyle\int_0^{\pi/2}\left[A(\theta) + B(\theta)\cos^2(\theta)\right]\sin(\theta)d\theta} \tag{59}$$

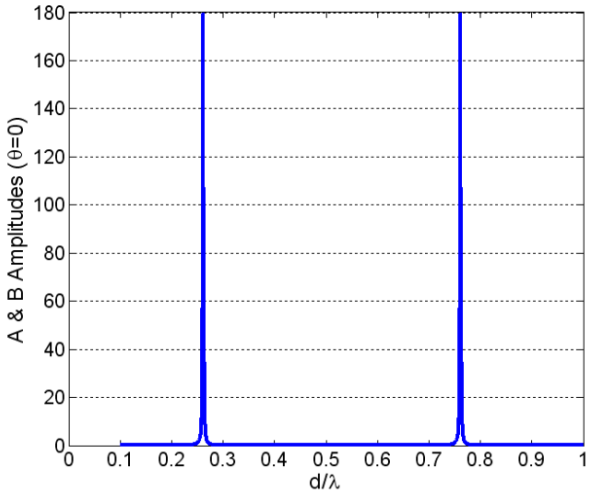

Figure 2. A and B amplitudes versus d/λ for $\theta = 0$, $r^{TE} = r^{TM} = .99e^{j\angle -172^\circ}$.

Also, the radiation resistance may be written as

$$R_r = \frac{2P_{rad}}{|I|^2} = \eta\frac{\pi}{2}\left(\frac{l}{\lambda}\right)^2 \int_0^{\pi/2} \left[A(\theta) + B(\theta)\cos^2(\theta)\right]\sin(\theta)d\theta \quad (60)$$

To compare, the x-directed electric dipole in free space has a radiation resistance of

$$R_r = \frac{2P_{rad}}{|I|^2} = \eta\frac{\pi}{2}\left(\frac{l}{\lambda}\right)^2 \times \frac{4}{3} \quad (61)$$

Because of the integral term of (60), the radiation resistance and consequently input resistance of antenna depend on the characteristics of PRS and their spacing. Therefore, we have additional parameters to adjust the input resistance of structure. This matter has already been studied for a structure excited by probe fed-microstrip antenna [17]. Compared to the x-directed infinitesimal electric dipole in free space, the two parameters A and B are included in the directivity of the structure from TE_z and TM_z components, respectively. These parameters depend on the reflection coefficients of PRS, spacing and the incident angle on them. As shown in Figures 2, 3 the necessary condition to achieve high directivity is near complete reflection coefficient in resonant frequency. This reflectivity is necessary for both polarizations of the incident plane waves (TEz and TMz) and

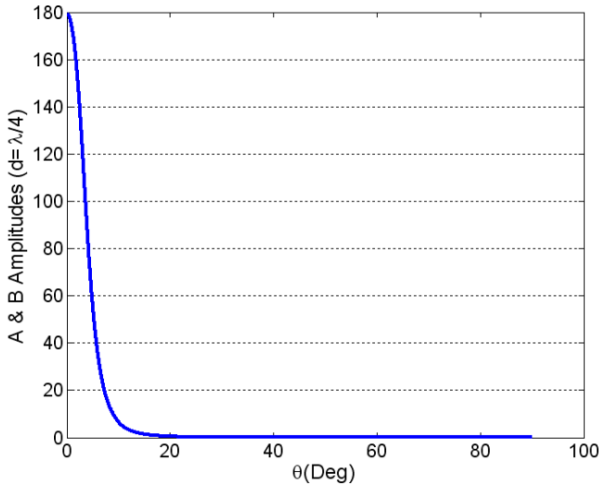

Figure 3. A and B amplitudes versus θ for $d = \lambda/4$, $r^{TE} = r^{TM} = .99e^{j\angle -172^\circ}$.

can be achieved by dielectric plates with very high permittivity which is commercially not easy obtain, multi layer dielectric plates as 1-D EBG which leads to thick PRS layer, and frequency selective surface as 2-D EBG. The PRSs that are designed with dielectric plates are polarization sensitive, especially for oblique incident angles. Therefore, the FSS structures are the best choice for the design of the required PRS [3,9,10,17]. In the following we assume that for a special frequency and any incident angle, the reflection coefficients for both TE_z and TM_z modes are equal. To study the effects of A and B factors, their variations are depicted versus (d/λ) in Figure 2 for normal incidence angle. As shown, there are resonance frequencies at which the amplitudes of A and B are maximum.

The resonance frequencies take place at $d = m\lambda/4, (m = 1, 3, 5 \ldots)$. At the first resonance $(d = \lambda/4)$, the A and B factors are examined versus incident angle θ in Figure 3.

At other resonance frequencies, we can obtain more resonance incident angles. This phenomenon leads to multiple beam radiation patterns, which are not desirable in broadside applications. This situation is shown in Figure 4 for $d = 3\lambda/4$.

In this case, we have two lobes in broadside and $\theta = 70^\circ$ directions. Figures 5 and 6 show the directivity of the structure for $\phi = 0$, $\frac{\pi}{4}$, $\frac{\pi}{2}$ planes and $d = \lambda/4$, $3\lambda/4$, respectively.

As observed, increasing the distance between PRS leads to multi-

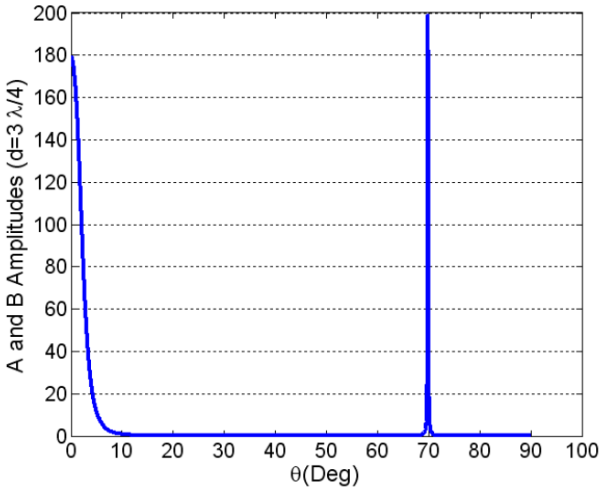

Figure 4. A and B amplitudes versus θ for $d = 3\lambda/4$, $r^{TE} = r^{TM} = .99e^{j\angle -172^\circ}$.

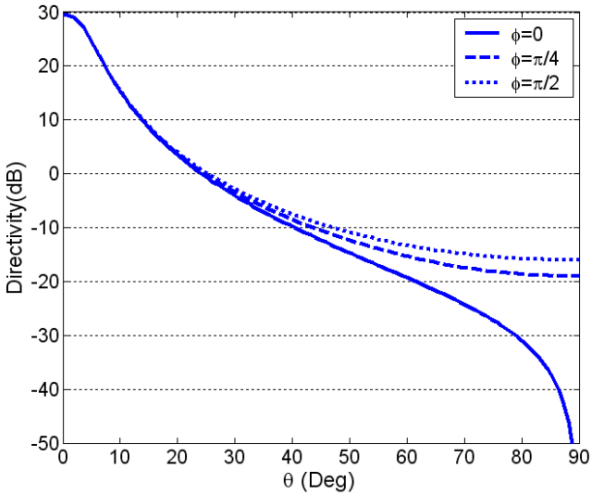

Figure 5. Directivity of structure versus θ for $d = \lambda/4$ and $\phi = 0$, $\frac{\pi}{2}$ and $\frac{\pi}{4}$ planes.

beam radiation from the structure. Also, at resonance frequencies the radiation resistance of the structure is more than the radiation resistance of the infinitesimal dipole in free space (Figure 8).

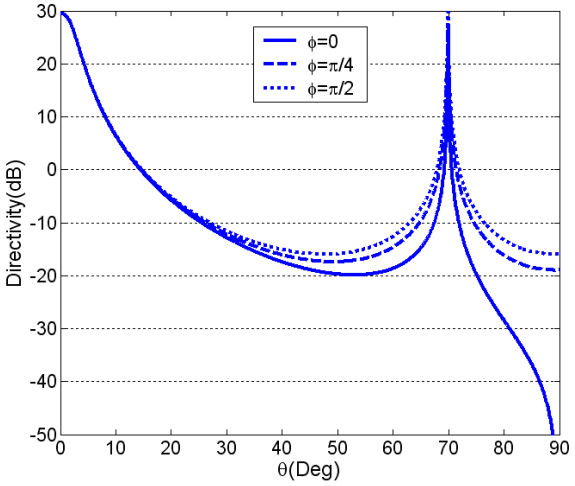

Figure 6. Directivity of structure versus θ for $d = 3\lambda/4$ and $\phi = 0$, $\frac{\pi}{2}$ and $\frac{\pi}{4}$ planes.

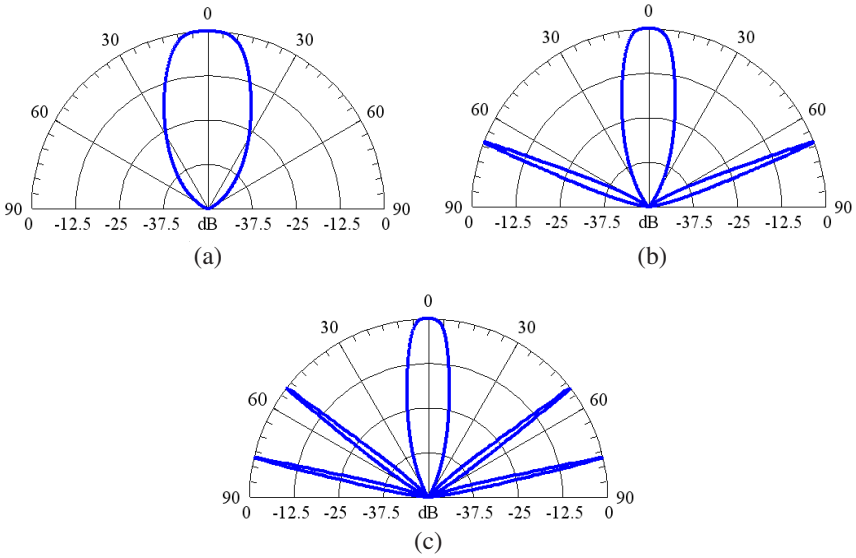

Figure 7. Radiation pattern of structure for upper half space and $r^{TE} = r^{TM} = .9e^{j\angle -154.15^{\circ}}$, (a) $d \approx \lambda/4$, (b) $d \approx 3\lambda/4$ and (c) $d \approx 5\lambda/4$.

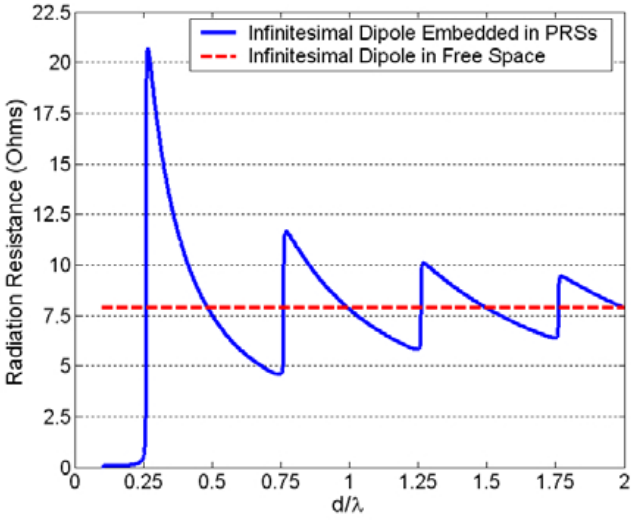

Figure 8. Radiation resistance of structure embedded between two PRS for $d = 3\lambda/4$, $r^{TE}=r^{TM}=.99e^{j\angle -172^\circ}$.

5. CONCLUSION

In this paper the far field radiation pattern of an infinitesimal dipole antenna as a prime source embedded between two PRS has been studied. This analytical study shows how a proper choice of the PRS reflectivity and spacing lead to directivity enhancement of the infinitesimal dipole. Also, the analytical results make it possible to study the effects of PRS on the radiation of different types of primary sources such as wire and aperture antennas.

APPENDIX A.

The general form of the far field approximation is $F(r, \theta, \phi) = f(\theta, \phi)\frac{e^{jkr}}{r}$. The derivations of r, θ and ϕ are given by Hence, the derivations of F with respective to x, y and z, using the chain rule,

	r	θ	ϕ
$\frac{\partial}{\partial x}$	$\sin\theta\cos\phi$	$\frac{\cos\theta\cos\phi}{r}$	$-\frac{\sin(\phi)}{r\sin(\theta)}$
$\frac{\partial}{\partial y}$	$\sin\theta\sin\phi$	$\frac{\cos\theta\sin\phi}{r}$	$\frac{\cos(\phi)}{r\sin(\theta)}$
$\frac{\partial}{\partial z}$	$\cos(\theta)$	$-\frac{\sin(\theta)}{r}$	0

become

$$\frac{\partial F}{\partial x} = \sin(\theta)\cos(\phi)\frac{\partial f}{\partial r} + \frac{\cos(\theta)\cos(\phi)}{r}\frac{\partial f}{\partial \theta} - \frac{\sin(\phi)}{r\sin(\theta)}\frac{\partial f}{\partial \phi} \quad \text{(A1)}$$

$$\frac{\partial F}{\partial y} = \sin(\theta)\sin(\phi)\frac{\partial f}{\partial r} + \frac{\cos(\theta)\sin(\phi)}{r}\frac{\partial f}{\partial \theta} + \frac{\cos(\phi)}{r\sin(\theta)}\frac{\partial f}{\partial \phi} \quad \text{(A2)}$$

$$\frac{\partial F}{\partial z} = \cos(\theta)\frac{\partial f}{\partial r} - \frac{\sin(\theta)}{r}\frac{\partial f}{\partial \theta} \quad \text{(A3)}$$

The derivations of (A1), (A2), and (A3) with respect to z are

$$\begin{aligned}\frac{\partial^2 F}{\partial z \partial x} &= \sin(\theta)\cos(\theta)\cos(\phi)\frac{\partial^2 f}{\partial r^2} - \sin^2(\theta)\cos(\phi)\frac{\partial}{\partial r}(\frac{1}{r}\frac{\partial f}{\partial \theta}) \\ &+ \frac{\cos(\theta)\cos(\phi)}{r}\frac{\partial}{\partial \theta}(\cos(\theta)\frac{\partial f}{\partial r}) - \frac{\cos(\theta)\cos(\phi)}{r^2}\frac{\partial}{\partial \theta}(\sin(\theta)\frac{\partial f}{\partial \theta}) \\ &- \frac{\cos(\theta)\sin(\phi)}{r\sin(\theta)}\frac{\partial^2 f}{\partial r \partial \phi} + \frac{\sin(\phi)}{r^2}\frac{\partial^2 F}{\partial \theta \partial \phi} \quad \text{(A4)}\end{aligned}$$

$$\begin{aligned}\frac{\partial^2 F}{\partial z \partial y} &= \sin(\theta)\cos(\theta)\sin(\phi)\frac{\partial^2 f}{\partial r^2} - \sin^2(\theta)\sin(\phi)\frac{\partial}{\partial r}(\frac{1}{r}\frac{\partial f}{\partial \theta}) \\ &+ \frac{\cos(\theta)\sin(\phi)}{r}\frac{\partial}{\partial \theta}(\cos(\theta)\frac{\partial f}{\partial r}) - \frac{\cos(\theta)\sin(\phi)}{r^2}\frac{\partial}{\partial \theta}(\sin(\theta)\frac{\partial f}{\partial \theta}) \\ &+ \frac{\cos(\theta)\cos(\phi)}{r\sin(\theta)}\frac{\partial^2 f}{\partial r \partial \phi} - \frac{\cos(\phi)}{r^2}\frac{\partial^2 F}{\partial \theta \partial \phi} \quad \text{(A5)}\end{aligned}$$

$$\begin{aligned}\frac{\partial^2 F}{\partial z^2} &= \cos^2(\theta)\frac{\partial^2 f}{\partial r^2} + \frac{\sin^2(\theta)}{r}\frac{\partial f}{\partial r} - \frac{2\sin(\theta)\cos(\theta)}{r}\frac{\partial f}{\partial r \partial \theta} \\ &+ \frac{2\sin(\theta)\cos(\theta)}{r^2}\frac{\partial f}{\partial \theta} + \frac{\sin^2(\theta)}{r}\frac{\partial^2 f}{\partial \theta^2} \quad \text{(A6)}\end{aligned}$$

For the far field approximation, the terms $\frac{1}{r^n}$ $n = 2, 3, \ldots$ are neglected, therefore the expressions (A1) to (A6) become

$$\frac{\partial^2}{\partial x \partial z}(\bullet) = -k^2 \sin(\theta)\cos(\theta)\cos(\phi)(\bullet) \quad \text{(A7)}$$

$$\frac{\partial^2}{\partial y \partial z}(\bullet) = -k^2 \sin(\theta)\cos(\theta)\sin(\phi)(\bullet) \quad \text{(A8)}$$

$$\frac{\partial^2}{\partial z^2}(\bullet) = -k^2 \cos^2(\theta)(\bullet) \quad \text{(A9)}$$

$$\frac{\partial}{\partial x}(\bullet) = jk \sin(\theta)\cos(\phi)(\bullet) \quad \text{(A10)}$$

$$\frac{\partial}{\partial y}(\bullet) = jk \sin(\theta)\sin(\phi)(\bullet) \quad \text{(A11)}$$

REFERENCES

1. Thevenot, M., C. Cheype, A. Reineix, and B. Jecko, "Directive photonic bandgap antennas," *IEEE, Transaction on Microwave Theory and Techniques*, Vol. 47, No. 11, 2115–2122, Nov. 1999.
2. Cheype, C., C. Serier, M. Thevenot, A. Reineix, and B. Jecko, "An electromagnetic bandgap resonator antenna," *IEEE Transactions on Antennas and Propagation*, Vol. 50, No. 9, 1285–1290, September 2002.
3. Maagt, P. D., R. Gonzalo, Y. C. Vardaxoglou, and J. M. Baracco, "Electromagnetic bandgap antennas and components for microwave and (sub) millimeter wave application," *IEEE Trans. Antennas and Propagation*, Vol. 51, No. 10, 2667–2677, 2003.
4. Chang, C. C., Y. Qian, and T. Itoh, "Analysis and applications of uniplanar compact photonic bandgap structures," *Progress In Electromagnetics Research*, PIER 41, 211–235, 2003.
5. Weily, A. R., K. P. Esselle, B. C. Sanders, and T. S. Bird, "High gain 1-D resonator antenna," *Microwave and Optical Technology Letters*, Vol. 47, No. 2, 107–114, October 2005.
6. Lee, Y. J. U., J. Yeo, K. D. Ko, R. Mittra, Y. Lee, and W. S. Park, "A novel design technique for control of defect frequencies of an electromagnetic bandgap (EBG) superstrate for dual-band directivity enhancement," *Microwave and Optical Technology Letters*, Vol. 42, No. 1, 25–31, July 2005.
7. Lee, Y. J. U., J. Yeo, R. Mittra, Y. Lee, and W. S. Park, "Application of electromagnetic bandgap (EBG) superstrates with controllable defect for a class of patch antennas as spatial angular

filters," *IEEE Transactions on Antennas and Propagation*, Vol. 53, No. 1, 224–235, January 2005.

8. Akalin, T., J. Danglot, O. Vanbesien, and Lippens, "A highly directive dipole antenna embedded in a Fabry-Perot type cavity," *IEEE Microwave and Wireless Components*, Vol. 12, No. 2, 48–50, February 2002.
9. Wang, S., A. P. Feresidis, G. Goussetis, and J. C. Vardaxoglou, "High-gain subwavelength resonant vavity antennas based on metamaterial ground plane," *IEE Proc. on Microwave, Antennas and Propagation*, Vol. 153, No. 1, February 2006.
10. Feresidis, A. P., G. Goussetis, S. Wang, and J. C. Vardaxoglou, "Artificial magnetic conductor surfaces and their application to low-profile high-gain planar antennas," *IEEE Transaction on Antennas and Propagation*, Vol. 53, No. 1, 209–215, January 2005.
11. Boutayeb, H. and T. A. Denidni, "Internally excited FabryCpérot type cavity: power normalization and directivity evaluation," *IEEE Antennas and Wireless Propagation Letters*, Vol. 5, 2006.
12. Boutayeb, H., K. Mahdjoubi, A. C. Tarot, and T. A. Denidi, "Directivity of an antenna embedded inside a Fabry-Perot cavity: analysis and design," *Microwave and Optical Technology Letters*, Vol. 48, No. 1, January 2006.
13. Boutayeb, H., K. Mahdjoubi, and A. C. Tarot, "Multi-layer crystal of metallic wires: analysis of the transmission coefficient for outside and inside excitation," *Progress In Electromagnetics Research*, PIER 59, 299–324, 2006.
14. Kong, J. A., *Electromagnetic Wave Theory*, Wiley Interscience, New York, 1990, EMW Publishing, Cambridge, 2000.
15. Kong, J. A., "Electromagnetic wave interaction with stratified negative isotropic media," *Progress In Electromagnetics Research*, PIER 35, 1–52, 2002.
16. Balanis, C., *Antenna Theory Analysis and Design*, John Wiely & Sons, New Jersey, 2005.
17. Pirhadi, A., M. Hakkak, and F. Keshmiri, "Using electromagnetic bandgap superstrate to enhance the bandwidth of probe-fed microstrip antenna," *Progress In Electromagnetics Research*, PIER 61, 215–230, 2006.